Fuel 232 (2018) 659–665

Contents lists available at ScienceDirect

Fuel

journal homepage: www.elsevier.com/locate/fuel

Full Length Article

Dynamics of methane/air premixed flame in a mesoscale diverging combustor with/without a cylindrical flame holder

Jianlong Wan, Cheng Shang, Haibo Zhao*

State Key Laboratory of Coal Combustion, School of Energy and Power Engineering, Huazhong University of Science and Technology, Wuhan 430074, China

ARTICLE INFO

Keywords:
Cylindrical flame holder
Diverging combustor
Flammability limit
Flame dynamics
Oscillating flame

ABSTRACT

A mesoscale diverging combustor with a cylindrical flame holder is developed to improve the flame stability and obtain the steadily symmetrical flame, which can be used as heat source for the mesoscale TPV (Thermophotovoltaic) system. The present work investigates the flammability limits based on equivalence ratio and the flame dynamics in the combustors with/without a cylindrical flame holder. For the combustor without the holder, four typical flame propagation modes, the stable slant, oscillating, spinning x-shape and flame blow-off, are observed, and all these flame patterns are asymmetrical. On the other side, the introduction of the cylindrical flame holder can significantly suppress the unstable flame and improve the flame stability probably due to enhanced flame-wall coupling and/or flow recirculation effects, as expected. The stable flame in the combustor with the holder can remain symmetrical under a quite wide range of equivalence ratio and the spinning x-shape mode does not occur here. Although the oscillating flames are also observed in relative narrow range of equivalence ratio in the combustor with the holder, their behaviors still keep symmetrical and their oscillating frequencies are probably dependent on the enhanced flame-wall coupling effect instead of the flame speed. In addition, the flame blow-off dynamics in the combustors with/without a cylindrical flame holder are also demonstrated and discussed in detail. In summary, the cylindrical flame holder can significantly improve the flame stability and makes the flame always remain symmetrical, which is beneficial for extensive application of the combustor with the diverging structure.

1. Introduction

Combustion in micro-/meso-scale combustors with relatively large surface area-volume ratios is easy to lose its stability because of the increased heat loss to the environment and the short residence time of gaseous mixture [1–5]. In some extreme cases, the flame instability may lead to the flame blow-off, flashback and structure damage. These problems result in various dynamic flame behaviors in the micro-/meso-scale combustors. The flame dynamics in the combustor with a constant channel width has been widely investigated, and some classical flame patterns were observed [6,7]. Maruta et al. [6] found the flame with repetitive extinction and ignition (FREI) in a narrow tube combustor with a temperature gradient, which was also numerically observed by Bucci et al. [7] via direct numerical simulation (DNS). Kurdyumov et al. [8] experimentally and numerically studied the premixed flame dynamics of methane/air around the flashback limit in a mesoscale tube, and they pointed out that the flame-wall coupling effect is responsible for the formation of multiple oscillatory flame behaviors. Pizza et al. [9] found five dynamic flame types which included periodic ignition and extinction, symmetric V-shaped, asymmetric, oscillating and oscillating flames in mesoscale plane channels via DNS, and these flame dynamic behaviors were also experimentally and numerically observed by Brambilla et al. [10]. These works mainly focused on the combustor with a constant channel width.

Most practical combustors have variable chamber width [11]. Some researchers have observed stable flame behaviors in the diverging plane and tubular combustors [11–14]. However, it is hard to obtain the symmetrically stable flame within a wide operating range of inlet velocity and equivalence ratio [13]. In fact, the variation of chamber width will affect the incoming flow velocity in the combustion chamber, which can dramatically influence the heat loss and flame-wall coupling effect [15]. As well known, the flame-wall coupling effect can significantly affect the flame propagation modes and flame structure, and it can lead to some unstable flames [16–19]. For example, Xu and Ju [11] studied the spinning flame in a mesoscale diverging tubular combustor experimentally and theoretically. They observed four propagation waves: the propagating flame, self-extinguished flame, stabilized planar flame and spinning flame. Moreover, they pointed out that

* Corresponding author at: State Key Laboratory of Coal Combustion, Huazhong University of Science and Technology, 1037 Luoyu Road, Wuhan 430074, China.
E-mail address: hzhao@hust.edu.cn (H. Zhao).

https://doi.org/10.1016/j.fuel.2018.06.026
Received 4 February 2018; Received in revised form 19 May 2018; Accepted 7 June 2018
0016-2361/ © 2018 Elsevier Ltd. All rights reserved.

the critical flow rate highly depends on the equivalence ratio when the flame begins to periodically spin. The spinning flame with high frequency was observed by Deshpande and Kumar [20] in a mesoscale tube combustors with two/three steps, and their results showed that the flow rate and equivalence ratio of methane/air are responsible for the formation of spinning flame. In addition, Akram and Kumar [13] investigated flame dynamics of methane/air premixed mixture in a mesoscale diverging combustor, and they observed three flame propagation modes: the planar flame, negatively stretched flame and positively stretched flame. Obviously, these unstable flame propagation modes impede the extensive application of the combustors with the diverging structure. In order to solve the above issues, Baigmohammadi et al. [21] pointed out that the wire insertion can significantly improve the flame stabilization in a micro combustor with backward facing step, which is ascribed to the flame-wire wall coupling effect. Recently, Yang et al. [22] found that the block insertion can obviously increase the mean wall temperature of the combustor with backward facing step and the flame stability. Porous media was also inserted into the combustion chamber to stabilize the flame via enhancing flame-solid coupling [23,24]. To sum up, the enhanced flame-wall coupling effect in the presence of flame holder can remarkably improve the flame stability in combustor.

Our research object is the tube combustor, which owns an axial symmetry structure. An inserted obstacle with the axial symmetry structure is more suitable for the tube combustor because the flame most likely presents axial symmetry behavior, which is convenient for experimental and numerical study. Therefore, in this paper, a cylindrical flame holder which can significantly enhance the flame-wall coupling is employed in the mesoscale diverging combustor to suppress the dynamic flame and improve flame stability. For the application in practice, this combustor which can provide steadily symmetrical flame in a wide operating range can be used as heat source for the mesoscale TPV (Thermophotovoltaic) system. For the theoretical aspect, this combustor can act as an universal model for further researching on the flame-wall coupling effect on the flame dynamics. The present combustor (no external heating) which is developed for the first time is easier to reproduce for the numerical analysis of the relative problem. Therefore, the flame dynamics in the combustors are reported in detail. In order to intuitively illustrate the effect of flame holder on improving flame stability, we also display the multiple flame dynamic behaviors in a mesoscale diverging combustor without a cylindrical flame holder.

2. Experimental

The experimental system is schematically presented in Fig. 1. Methane and air are fully mixed in a mixing tank before entering the combustor via stainless steel pipe of 1/4 in.. A flame gun is applied to ignite the unburned mixture at the exit of the combustor. A digital video camera (Canon EOS 6D with the recording frequency of 50 Hz) is used to take photographs with a shutter speed of 1/180 s and to capture videos of flame dynamics. We manufacture two mesoscale diverging combustors using the quartz glass with a thermal conductivity of 2.0 W/(m·K), one with a cylindrical flame holder and another without. The geometry of two diverging combustors is same. Here we just present the geometrical structure of the combustor with holder in Fig. 1. The cross-section of combustor is a circle. The wall thickness (δ) is 1.0 mm. The diameter of the cylindrical flame holder is 2.0 mm, and the gap distance between the flame holder and inner wall at the inlet of combustor is 1.0 mm. The total height of the combustor is 150.0 mm. For the sake of a clear description, the whole combustor channel is divided into three segments, namely, the inlet section (20δ), the diverging section (30δ) and the straight section (100δ). In addition, Fig. S1 in Supplementary Materials (SM) shows the three-dimensional geometry of this combustor.

In this work, we change the equivalence ratio of fuel mixture under a constant inlet velocity. We firstly ignite the fresh mixture under an inlet velocity at $\phi = 1.0$, which makes flame stabilized in the diverging section of combustor, and then increase or decrease the equivalence ratio with a step of 0.025 until flame blows off under a constant inlet velocity.

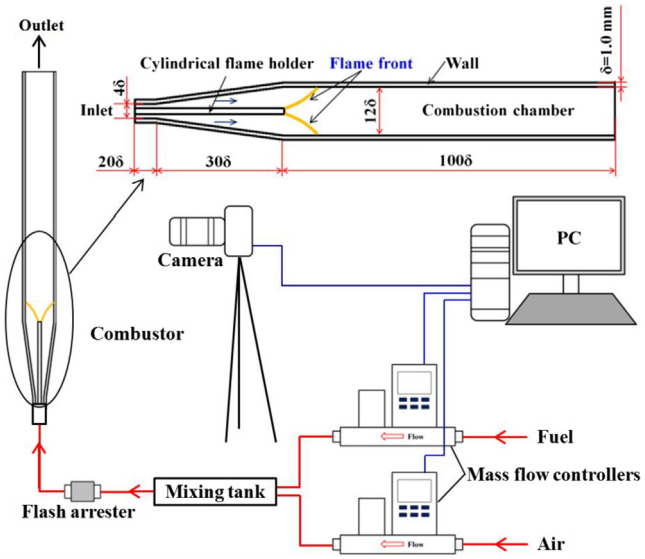

Fig. 1. Schematic view of the experimental system.

Three flow rates (Q_{in}) are adopted, which are 1.128 L/min, 1.413 L/min and 1.698 L/min, respectively. The corresponding inlet velocities (V_{in}) in the diverging combustor without the cylindrical flame holder (CWO) are 1.50 m/s, 1.875 m/s and 2.25 m/s, respectively. With respect to the diverging combustor with flame holder (CW), the corresponding V_{in} are 2.0 m/s, 2.5 m/s and 3.0 m/s, respectively. Each case is repeated three times, and the differences of each one are small. In addition, it should be pointed out that the error bar in the most following figures comes from the environment perturbation (such as the perturbation of heat loss coefficient) rather than the measurement.

3. Results and discussion

3.1. Flame regime diagrams

The regime diagram of CH_4/air premixed flame patterns in CWO is presented in Fig. 2a. In the absence of the flame holder, the flammability limits at different flow rates are almost same, but the distribution characteristics of flame patterns are different. For a smaller or larger flow rate, the stable slant flames only occur around the stoichiometric ratio ($0.925 \le \phi \le 1.175$ for $Q_{in} = 1.128$ L/min, $0.850 \le \phi \le 1.150$ for $Q_{in} = 1.698$ L/min). Under a moderate flow rate ($Q_{in} = 1.413$ L/min), interestingly the flame restores stabilization when the equivalence ratio decreases from 0.750 to 0.700 or increases from 1.250 to 1.300. We suppose that the flame speed under an intermediate flow rate which provides a moderate heat release rate can reach a static balance with the flow velocity in the diverging section at a smaller or larger equivalence ratio. This re-stabilization phenomenon was also observed in the premixed flame under a step-wise wall temperature by Kurdyumov et al. [25]. Moreover, there is spinning x-shape flame at $Q_{in} = 1.128$ L/min and $Q_{in} = 1.698$ L/min, which does not occur at $Q_{in} = 1.413$ L/min. The oscillating flame appears at $Q_{in} = 1.413$ L/min and $Q_{in} = 1.698$ L/min, but is absent at $Q_{in} = 1.128$ L/min. In summary, at $Q_{in} = 1.128$ L/min, the stable flame transforms to spinning x-shape flame at first and then blows off with the increase or decrease of equivalence ratio from the stoichiometric ratio. At $Q_{in} = 1.413$ L/min, the stable flame transforms to oscillating flame at first and then recovers stabilization again. At $Q_{in} = 1.698$ L/min, with the increase of equivalence ratio, the stable flame becomes oscillating flame at first and

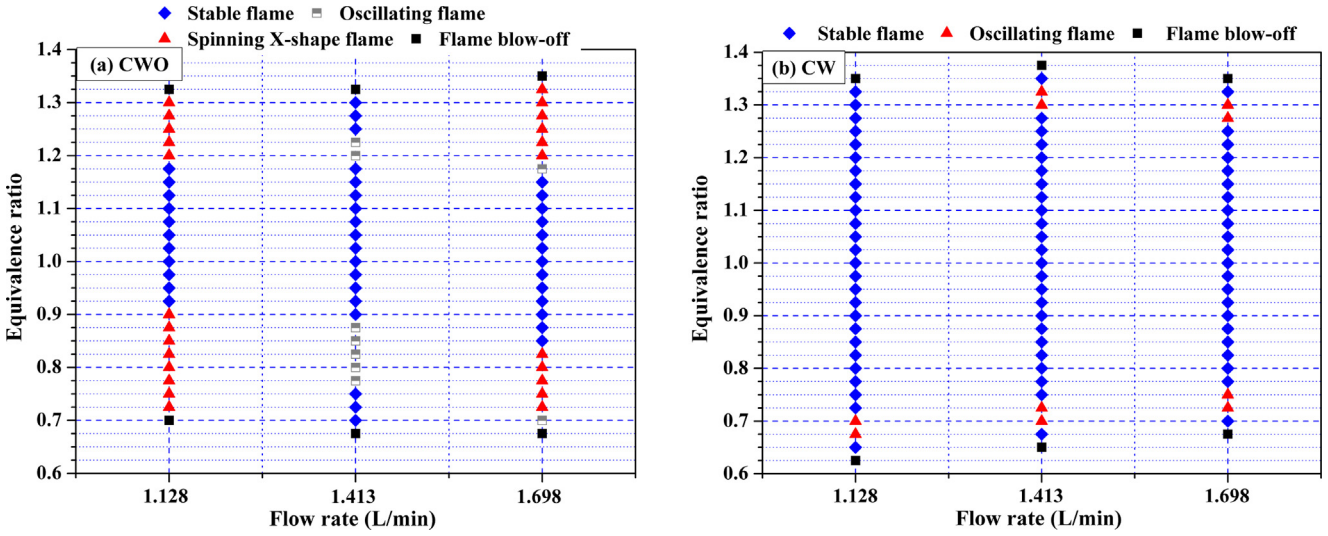

Fig. 2. Regime diagram of flame patterns in the CWO (a) and CW (b) for different flow rate and equivalence ratio.

then turns into spinning x-shape flame. As for the decreasing process of equivalence, the stable flame becomes spinning x-shape flame at first and then turns into oscillating flame. These dynamic flame behaviors for different flow rates are similar, but their oscillating frequencies and amplitudes differ quite considerably, which will be quantitatively discussed in the following sections.

Fig. 2b shows the regime diagram of flame patterns in CW. It can be seen that flame can remain symmetrically stable in a quite wide range of the equivalence ratio. Additionally, the spinning x-shape flame does not occur in CW, and the oscillating flame along with the vertical wall of flame holder in CW is almost symmetrical. We also observe the flame re-stabilization phenomenon before the flame blows off at three flow rates, which might be related to the anchoring effect of recirculation zone or low velocity zone behind the flame holder as the flame roots attach to the end wall of the flame holder. In summary, at Q_{in} = 1.128 L/min, the stable flame becomes oscillating flame at first and then recovers stable with the decrease of equivalence ratio from the stoichiometric ratio. At Q_{in} = 1.413 L/min and 1.698 L/min, with the increase or decrease of equivalence ratio, the stable flame also transforms to oscillating mode firstly and then recovers stable again. Besides, the flammability limits are indeed expanded in CW. These results imply that the flame holder can significantly suppress the unstable flame in the diverging combustor. Having all possible flame patterns at Q_{in} = 1.698 L/min in CWO and CW, their characteristics versus the equivalence ratio are displayed and discussed in the following part.

3.2. Stable flame in CWO and CW

In order to confirm every stable flame is really completely static, we shot the stable flame for a long time, and Fig. S2 in SM indicates that the stable flame is actually completely static. Fig. 3 presents the locations of flame root and top, the height of flame front. In this paper, the locations of flame root (L_r) and flame top (L_t) are read based on the inlet of the diverging section (the white horizontal dash line in Fig. 3), and the difference in the locations of flame top and root is the height of flame front. The error bar in the figure is from flame fluctuation caused by environment perturbation. There are three observations: (1) Both the flame root and top shift upstream (*i.e.*, closer to the inlet of combustor) firstly and then downstream with a decreasing equivalence ratio, and the flame is most adjacent to the combustor inlet at ϕ = 1.050. (2) As the decrease of equivalence ratio, the flame height decreases at first and then increases, and it also reaches the minimum at ϕ = 1.050. It can be read that the minima of flame height at V_{in} = 1.500 m/s, 1.875 m/s and 2.250 m/s are 7.4 mm, 8.9 mm and 11.0 mm, respectively. (3) With the decrease of V_{in}, the flame root and top significantly move upstream, and the flame is shortened under the same ϕ.

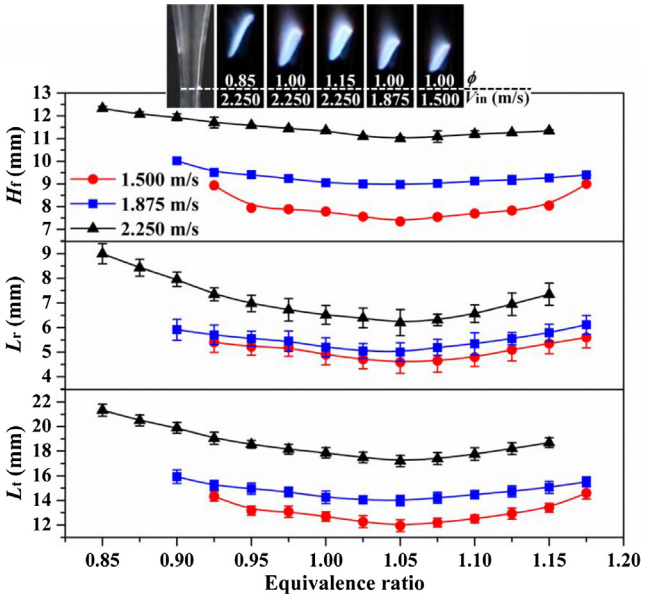

Fig. 3. The locations of flame root (L_r) and flame top (L_t), the height of flame front (H_f) for stable behaviors at different equivalence ratios and inlet velocities in CWO.

In the presence of the flame holder, the flame can remain symmetrically stable within a wide range of equivalence ratio (see Fig. 4), and the top-view from the combustor exit presents the circular ring. This is probably because the flame holder is heated by the high temperature gaseous mixture (it is blazing in Fig. 4), and the flame root attaches to the vertical wall of flame holder so that the flame-wall coupling effect can be remarkably enhanced. As a result, the flame stabilization is significantly improved. Similarly, the flame shifts upstream firstly and then downstream with a decreasing equivalence ratio; the flame is located at the most upstream at ϕ = 1.050 because the flame speed in this case is the fastest [26]. It can be read that the most upstream locations of flame roots at ϕ = 1.050 for V_{in} = 2.0 m/s, 2.5 m/s and 3.0 m/s are 11.7 mm, 12.7 mm and 14.1 mm, respectively.

As mentioned in Fig. 2b, there also is re-stabilization phenomenon for each inlet velocity under a specific equivalence ratio (e.g.,

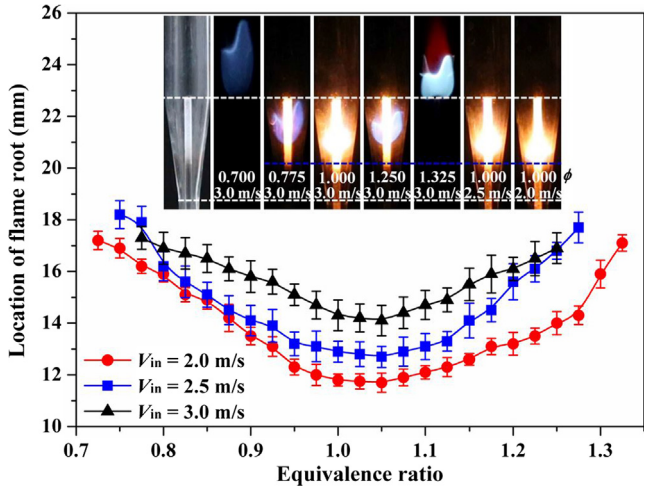

Fig. 4. The locations of flame roots for stable flame behavior at different equivalence ratio and inlet velocity in CW.

$\phi = 0.700$ and 1.325 at $V_{in} = 3.0$ m/s; $\phi = 0.675$ and 1.350 at $V_{in} = 2.5$ m/s; $\phi = 0.650$ at $V_{in} = 2.0$ m/s). It is the re-establish of the balance between flame speed and flow rate in the straight section that contributes to the phenomenon. Although the temperatures of the flame holder and combustor wall are not measured, we conjecture from Fig. 4 that the flame holder temperature at $\phi = 0.700$ and 1.325 is relatively low since the flame holder is nearly invisible. We suppose that the flame root is anchored by the recirculation zone behind the flame holder instead of the vertical wall of flame holder described above. The fuel-rich flame is brighter than that of fuel-lean, and the flame height of fuel-rich is shorter. Overall, the intuitive observations indicate that the flame holder can obviously improve the flame stability possibly due to the enhanced flame-wall coupling effect (for normal stable flames) or flow recirculation zone behind the flame holder (for re-stabilized flames).

3.3. Oscillating flame in CWO and CW

As well known, if a perturbation such as non-equilibrium heat loss or hydrodynamics instability breaks the static balance between the flame speed and the incoming flow velocity, some unstable flame propagation modes will occur. Fig. 5 shows that the slant flame in the absence of the holder is oscillating up and down at $\phi = 0.700$. Differently, the oscillating flame at $\phi = 0.700$ is almost within the straight section with a frequency of 5.56 Hz, but the flame at $\phi = 1.175$ is oscillating near the middle of diverging section with a faster oscillating frequency (16.67 Hz, see Fig. S3 in SM). This is mainly because that the

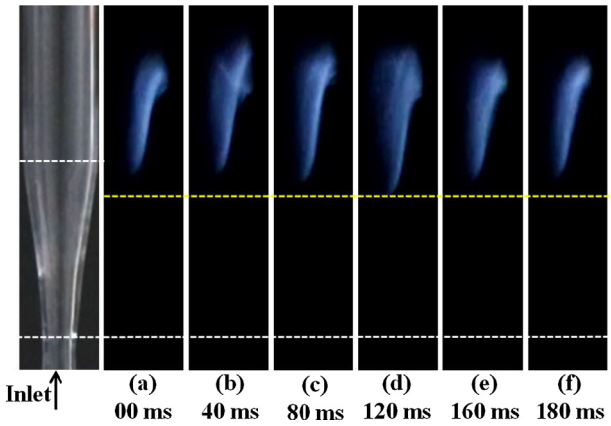

Fig. 5. The asymmetrically oscillating flame at $\phi = 0.700$ in one cycle for $V_{in} = 2.25$ m/s in CWO.

normal component of incoming flow velocity continuously adjusts with the flame speed in the diverging section. In addition, the oscillating amplitudes (the difference between the highest and lowest locations) of flame root, flame top, and flame height at $\phi = 0.700$ are obviously larger than that at $\phi = 1.175$. This is because the flame stability at $\phi = 0.700$ is weaker due to a lower wall temperature and a larger surface area of flame front.

In the presence of the holder, the oscillating flame is nearly symmetrical, as shown in Fig. 6. For the case of $\phi = 0.750$ ($V_{in} = 3.0$ m/s), the flame top which is close to the inner wall of combustor straight section is nearly fixed at the same location, which is probably ascribed to strong flame-wall coupling effect and relatively low flow velocity in the straight section (which is beneficial for achieving a static balance between the flow velocity and the flame speed). However, the flame root is oscillating down and up, because the flame front is continuously adjusting to make the flame speed approach the normal component of flow velocity, as shown in Fig. 6b. It is known that $V_{in,n} = S_L$ is the necessary condition for flame stabilization. From Fig. 6b, $V_{in,n} = V_{in} \times \cos\theta$, where $V_{in,n}$ is the normal component of the incoming flow velocity, θ is the acute angle between the flame speed and flow direction. When the equivalence ratio decreases to 0.75 or increases to 1.275, the burning velocity is decreasing at the same time, which leads to the movement of flame front from the location 1 to the downstream channel by the incoming unburned mixture. When the upstream boundary of flame front is at 1′-location, even through the cosθ is increasing, the incoming flow velocity is decreasing at the meantime due to a larger flow area, and the comprehensive effect makes the $V_{in,n}$ decrease. As a result, S_L is larger than $V_{in,n}$, which makes the upstream boundary of flame front return to a more upstream location. This oscillating phenomenon periodically occurs with time. In addition, even though the flame speed at $\phi = 1.275$ (26.1 cm/s) is faster than that at $\phi = 0.725$ (21.1 cm/s) under normal environment [26], their oscillating frequencies are almost same (~12 Hz), which means that the oscillating frequency in CW might be determined by the enhanced flame-wall coupling effect rather than the flame speed.

3.4. Spinning x-shape flame in CWO

As mentioned in Fig. 2, the spinning x-shape flame only exists in CWO. Fig. 7 shows the flame dynamics at $\phi = 0.825$ and $V_{in} = 2.25$ m/s (as a typical case), which presents that the flame is spinning left and right with a frequency of 12.5 Hz, and it locates in the diverging section of combustor. This flame propagation mode is similar to those reported by Xu and Ju [11] and Pizza et al. [9]. In their works, they also found the spinning x-shape flame, which attributes to the strong flame-wall coupling effect [11]. Moreover, Deshpande and Kumar [20] pointed out that the transition between the spinning flame and stable flame is significantly affected by the wall temperature, and the flame-wall coupling effect actually results in the appearance of the spinning x-shaped flame. Concretely, the flame has a tendency to shift downstream owing to the incoming flow, but the flame-wall coupling effect is trying to keep the flame stabilized at the same location. This competitive effect between them induces the appearance of the spinning x-shape flame. The spinning frequency is decreasing with a decrease in the equivalence ratio under lean fuel, which is ascribed to the decreasing flame speed [11].

3.5. Flame blow-off dynamics in CWO

At $V_{in} = 2.25$ m/s, when the equivalence ratio decreases to 0.675 or increases to 1.350, the flame will blow off due to the small flame speed and heat release rate. Figs. 8 and 9 present the dynamic processes for the two cases. At $\phi = 0.675$, the flame is oscillating up and down at first (the first stage of flame bow-off dynamics). The reasons for this flame propagation mode are following: at first, a larger flame surface area leads to a slower burning velocity, so the flame front is pushed downstream by the incoming fresh mixture (from $t = 0$ ms to 180 ms).

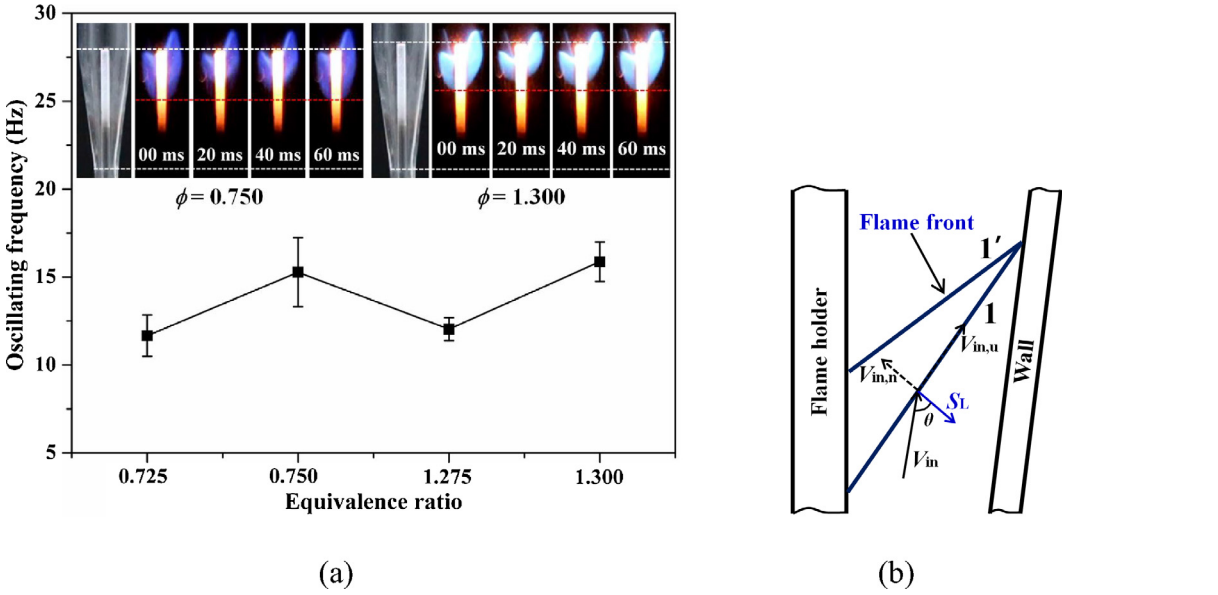

Fig. 6. The oscillating frequencies of symmetrically oscillating flame for one oscillating cycle at ϕ = 0.750, 0.750, 1.275 and 1.300 for V_{in} = 3.0 m/s in CW (a); the schematic of the oscillating behavior in CW (b).

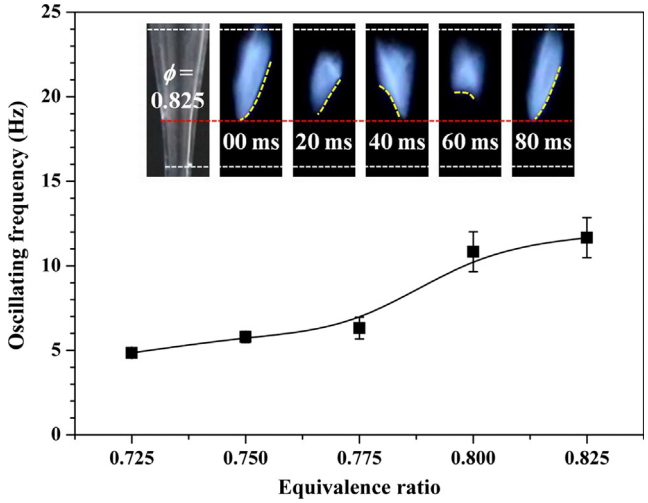

Fig. 7. The spinning frequencies of spinning x-shaped flame for different equivalence ratios under lean fuel at V_{in} = 2.25 m/s in CWO.

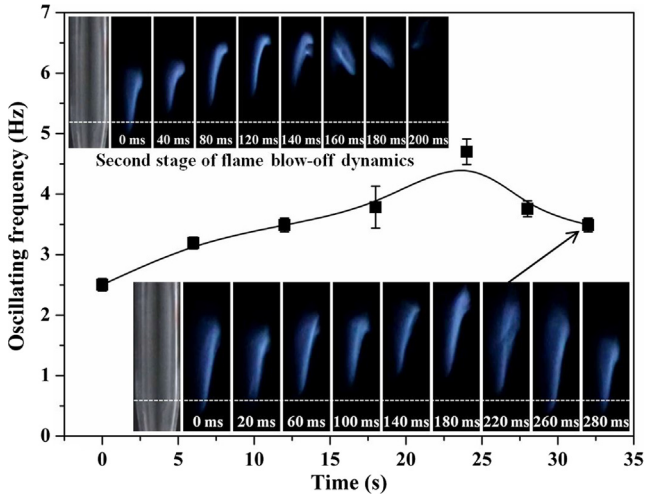

Fig. 8. The oscillating frequencies of the first stage at different time points and the second stage of flame blow-off dynamics under the conditions of ϕ = 0.675 and V_{in} = 2.25 m/s in CWO.

However, a larger flow area in the straight channel section results in a smaller incoming flow velocity, so a relative faster burning velocity combining the flame-wall coupling make the flame shift upstream (from t = 180 ms to 280 ms). Interestingly, the oscillating frequency increases firstly and then decreases with time. This is the competitive result among the flame-wall coupling effect, flame speed and oscillating amplitude. In the end, the incoming unburned mixture pushes the flame downstream at first (from t = 0.0 ms to 120 ms, the second stage in Fig. 8), and then the flame front becomes smaller (from t = 120 ms to 200 ms) probably due to a larger heat loss. Subsequently, the flame blows off.

At ϕ = 1.350, the flame is firstly oscillating around the centre of flame front (the first stage), as depicted in Fig. 9. It is noteworthy that the flame begins to oscillate after t = 47.00 s (the second half of the first stage), accompanying with fuel leak. The open fire at the exit of combustor is observed. Obviously, the redundant fuel exhausts along with high-temperature flue gas combusts again with the help of air near the combustor exit. This oscillating flame behavior, which appears like a regular limit cycle, is very similar to that observed by Pizza et al. [9] via direct numerical simulation. The present flame propagation mode connects the two asymmetric solutions (the inclining flame behaviors of left and right), which is attributed to a global bifurcation (heteroclinic connection). Moreover, the fuel leak occurs only in the first half of one oscillating period (from t = 0 ms to 60 ms), *i.e.*, the fuel leaks when the flame shrinks smaller. In addition, Fig. 9 indicates that the flame oscillating frequency is decreasing with time. This is mainly because that the flame speed is decreasing due to heat loss and the oscillating amplitude is increasing with time (see Fig. S4 in SM). After the first stage, the flame root and top shift toward each other (see Fig. 9), and this continuously reduced flame is finally extinguished due to heat loss.

3.6. Flame blow-off dynamics in CW

The flame blow-off dynamics under lean fuel and rich fuel are very similar in CW. Fig. 10 shows the location profiles of flame root in the first stage and second stage of flame blow-off dynamics at ϕ = 1.350. At first, the flame slowly shifts downstream with an almost constant displacement speed of 0.12 mm/s (from t = 0.0 s to 75.74 s), and the

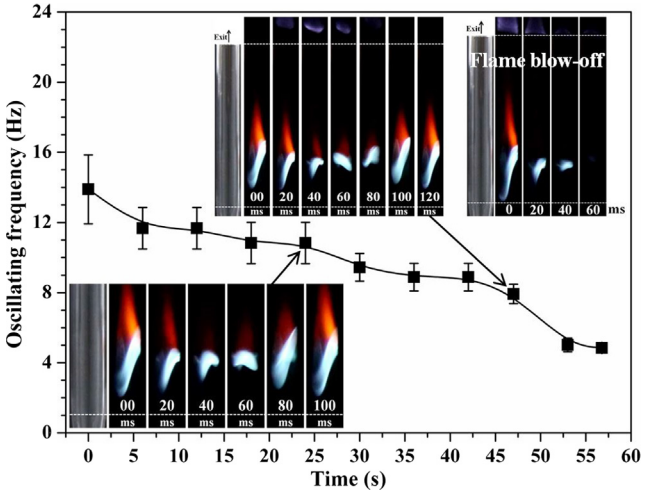

Fig. 9. The oscillating frequencies of the oscillating behavior (the first stage) and the second stage (flame blow-off) in the flame blow-off dynamic at different time points at $\phi = 1.350$ and $V_{in} = 2.25$ m/s in CWO.

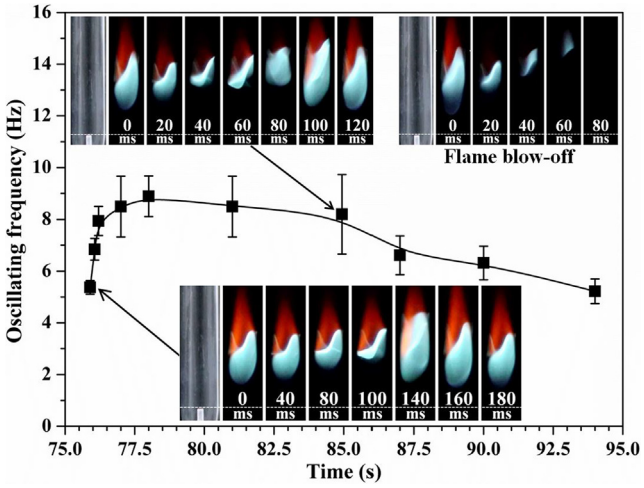

Fig. 11. The oscillating frequencies of the oscillating mode with asymmetric behavior (the third stage) and the last stage (flame blow-off) of flame blow-off dynamics for different time points at $\phi = 1.350$ and $V_{in} = 3.0$ m/s in CW.

height of flame front nearly remains unchanged. The flame keeps symmetrical even the flame is away from the flame holder, which means that the flame behavior is still significantly influenced by the symmetrical structure of flow field behind the flame holder instead of the flame-wall coupling effect of flame holder. Then, the flame starts to oscillate with the amplitude of 3.9 mm (the second stage). It can be seen that the flame top near the combust wall nearly remains at the same location, but the center of flame front shifts downstream firstly and then returns back. The reasons of the pulsating center can be got in Fig. 10b. At first, the larger curvature of flame front (1-location in Fig. 10b, $t = 00$ ms in Fig. 10a) leads to a larger heat loss. As a result, the burning velocity near upstream boundary is further decreasing, which induces the incoming unburned mixture to push the center downstream (from 1-location to 1′-location). In this moving process, the decreasing curvature of flame front gives rise to an increasing burning velocity. At the 1′-location in Fig. 10b ($t = \sim 40$ ms in Fig. 10a), the S_L is nearly equal to the V_{in}. However, the inertial effect makes the center zone of flame front continuously shift to a more downstream location (1″-location in Fig. 10b, $t = 80$ ms in Fig. 10a), which makes a larger S_L comparing with the V_{in}. Then, the center zone of flame front restores to a more upstream location again ($t = 160$ ms in Fig. 10a). Subsequently, as the solid wall temperature further decreases with time, the oscillating flame with asymmetry behavior appears after one cycle of the symmetrically oscillating mode (see Fig. 11).

Fig. 11 displays the oscillating frequencies of the oscillating flame with asymmetric behavior at $\phi = 1.350$, which is very similar to the case at $\phi = 0.675$ and $V_{in} = 2.25$ m/s in CWO (see Fig. 8), *i.e.*, and the oscillating frequency increases firstly and then decreases with time. In this stage, the flame becomes more disordered due to the decreasing wall temperature. After the third stage, the flame blows off, as presented in Fig. 11. In the last stage, the flame becomes smaller and smaller and moves toward the combustor exit at the same time. In the end, the flame is completely extinguished in the downstream combustion chamber.

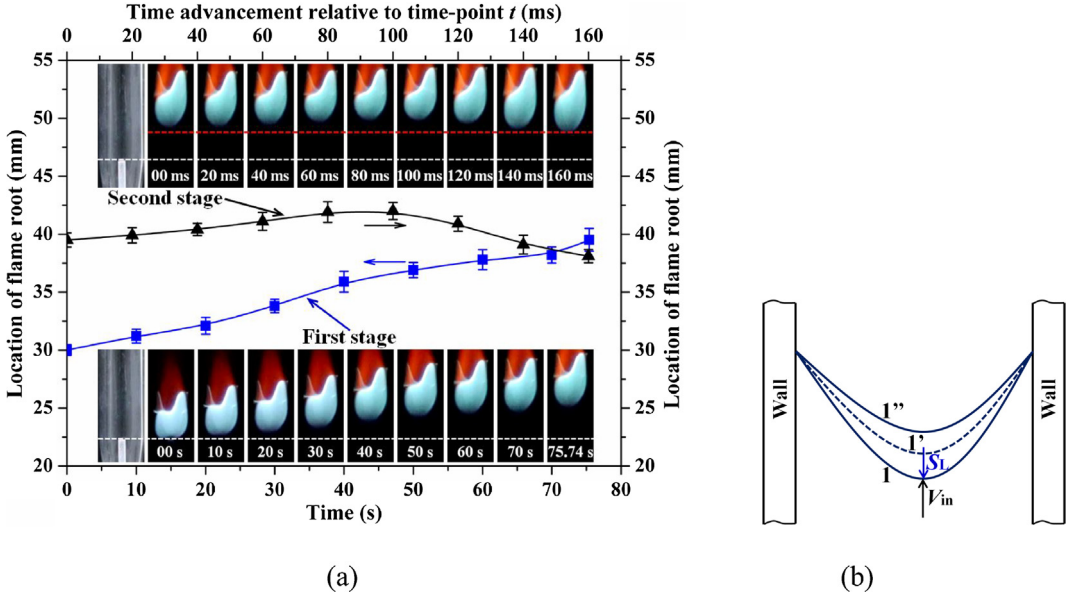

Fig. 10. The locations of flame roots in the first stage (the flame shifts downstream, from $t = 0.0$ s to $t = 75.74$ s) and the second stage (the symmetrically oscillating mode, from $t = 75.74$ s to $t = 75.79$ s) of flame blow-off dynamics at $\phi = 1.350$ and $V_{in} = 3.0$ m/s in CW (a); the schematic of the oscillating behavior at the second stage in CW (b).

4. Conclusions

A mesoscale diverging combustor with/without a cylindrical flame holder is developed in present work. The flammability limits and the flame dynamics in CWO and CW are investigated experimentally for three typical flow rates. The flame pattern diagrams of the stable slant flame, oscillating flame, spinning x-shape flame and flame blow-off are obtained as functions of the equivalence ratio and inlet velocity in CWO. For the stable slant flame, the flame shifts upstream to the inlet of combustor firstly and then downstream with the decrease of equivalence ratio (the flame at $\phi = 1.050$ is closest to the inlet of combustor), and the flame height varies accordingly. When the equivalence ratio decreases or increases to certain value, the asymmetrically oscillating flame or spinning x-shape flame appears. With a further increase or decrease in the equivalence ratio, the flame blows off, and the difference in the frequencies of oscillating modes in flame blow-off dynamics probably depends on the competitive effect of flame-wall coupling, flame speed and oscillating amplitude. However, the spinning x-shape flame does not occur in CW, and the oscillating flame in CW is almost symmetrical. The flame re-stabilization phenomena are observed at each inlet velocity. The flame can remain symmetrical for a quite wide range of equivalence ratio probably due to the enhanced flame-wall coupling effect. In a relative narrow range of equivalence ratio under lean or rich mixture, the flame presents symmetrically oscillating behavior, and its oscillating frequency is probably determined by the enhanced flame-wall coupling effect rather than the flame speed. In addition, the oscillating flame is also observed in the process of flame blow-off dynamics, and the oscillating frequency increases firstly and then decreases with time.

In summary, these results indicate that the asymmetrical dynamic flame observed in CWO can well be suppressed by the cylindrical flame holder, which means that the flame stability is significantly improved in CW. The simple structures of CWO and CW are convenient for researchers to carry out relevant numerical simulation study on the present experimental observations to understand the flame-wall coupling effect on flame dynamics better in future.

Acknowledgements

This work was supported by the Natural Science Foundation of China (Nos. 51706080, 51522603) and the China Postdoctoral Science Foundation (2016M600591, 2018T110761).

Appendix A. Supplementary data

Supplementary data associated with this article can be found, in the online version, at http://dx.doi.org/10.1016/j.fuel.2018.06.026.

References

[1] Ju Y, Maruta K. Microscale combustion: technology development and fundamental research. Prog Energy Combust Sci 2011;37(6):669–715.
[2] Pizza G, Frouzakis CE, Mantzaras J, Tomboulides AG, Boulouchos K. Dynamics of premixed hydrogen/air flames in mesoscale channels. Combust Flame 2008;155(1–2):2–20.
[3] Fernandez-Pello AC. Micro power generation using combustion: issues and approaches. Proc Combust Inst 2002;29:883–99.
[4] Yang W, Chou S, Chua K, An H, Karthikeyan K, Zhao X. An advanced micro modular combustor-radiator with heat recuperation for micro-TPV system application. Appl Energy 2012;97:749–53.
[5] Maruta K. Micro and mesoscale combustion. Proc Combust Inst 2011;33(1):125–50.
[6] Maruta K, Kataoka T, Kim NI, Minaev S, Fursenko R. Characteristics of combustion in a narrow channel with a temperature gradient. Proc Combust Inst 2005;30(2):2429–36.
[7] Bucci MA, Robinet J-C, Chibbaro S. Global stability analysis of 3D micro-combustion model. Combust Flame 2016;167:132–48.
[8] Kurdyumov V, Fernández-Tarrazo E, Truffaut JM, Quinard J, Wangher A, Searby G. Experimental and numerical study of premixed flame flashback. Proc Combust Inst 2007;31(1):1275–82.
[9] Pizza G, Frouzakis CE, Mantzaras J, Tomboulides AG, Boulouchos K. Dynamics of premixed hydrogen/air flames in microchannels. Combust Flame 2008;152(3):433–50.
[10] Brambilla A, Frouzakis CE, Mantzaras J, Bombach R, Boulouchos K. Flame dynamics in lean premixed/air combustion in a mesoscale channel. Combust Flame 2014;161(5):1268–81.
[11] Xu B, Ju Y. Experimental study of spinning combustion in a mesoscale divergent channel. Proc Combust Inst 2007;31(2):3285–92.
[12] Nair A, Velamati RK, Kumar S. Effect OF CO2/N2 dilution on laminar burning velocity of liquid petroleum gas-air mixtures at elevated temperatures. Energy 2016;100:145–53.
[13] Akram M, Kumar S. Experimental studies on dynamics of methane–air premixed flame in meso-scale diverging channels. Combust Flame 2011;158(5):915–24.
[14] Khandelwal B, Kumar S. Experimental investigations on flame stabilization behavior in a diverging micro channel with premixed methane–air mixtures. Appl Therm Eng 2010;30(17–18):2718–23.
[15] Ju Y, Xu BO. Effects of channel width and lewis number on the multiple flame regimes and propagation limits in mesoscale. Combust Sci Technol 2006;178(10–11):1723–53.
[16] Ju Y, Xu B. Theoretical and experimental studies on mesoscale flame propagation and extinction. Proc Combust Inst 2005;30(2):2445–53.
[17] Veeraragavan A. On flame propagation in narrow channels with enhanced wall thermal conduction. Energy 2015;93:631–40.
[18] Miguel-Brebion M, Mejia D, Xavier P, Duchaine F, Bedat B, Selle L, et al. Joint experimental and numerical study of the influence of flame holder temperature on the stabilization of a laminar methane flame on a cylinder. Combust Flame 2016;172:153–61.
[19] Mejia D, Miguel-Brebion M, Ghani A, Kaiser T, Duchaine F, Selle L, et al. Influence of flame-holder temperature on the acoustic flame transfer functions of a laminar flame. Combust Flame 2018;188:5–12.
[20] Deshpande AA, Kumar S. On the formation of spinning flames and combustion completeness for premixed fuel–air mixtures in stepped tube microcombustors. Appl Therm Eng 2013;51(1–2):91–101.
[21] Baigmohammadi M, Sarrafan Sadeghi S, Tabejamaat S, Zarvandi J. Numerical study of the effects of wire insertion on CH4(methane)/AIR pre-mixed flame in a micro combustor. Energy 2013;54:271–84.
[22] Yang WM, Jiang DY, Chua KYK, Zhao D, Pan JF. Combustion process and entropy generation in a novel microcombustor with a block insert. Chem Eng J 2015;274:231–7.
[23] Li J, Chou SK, Li ZW, Yang WM. Experimental investigation of porous media combustion in a planar micro-combustor. Fuel 2010;89(3):708–15.
[24] Li J, Wang Y, Shi J, Liu X. Dynamic behaviors of premixed hydrogen–air flames in a planar micro-combustor filled with porous medium. Fuel 2015;145:70–8.
[25] Kurdyumov VN, Pizza G, Frouzakis CE, Mantzaras J. Dynamics of premixed flames in a narrow channel with a step-wise wall temperature. Combust Flame 2009;156(11):2190–200.
[26] Chen Z. On the accuracy of laminar flame speeds measured from outwardly propagating spherical flames: methane/air at normal temperature and pressure. Combust Flame 2015;162(6):2442–53.